PYROXFERROITE BREAKDOWN TEXTURES IN APOLLO 12 BASALT. Borden, M.W.[1] Cronberger, K. and Neal, C.R.[1] [1]University of Notre Dame, Notre Dame IN, 46556; mborden2@nd.edu.

Introduction: Symplectite breakdown textures of pyroxferroite have been observed in Apollo 12 pigeonite basalt 12031 (thin sections 40 and 45 using backscatter electron microscopy (BSE); Figs. 1 and 2).. Previous studies on 12031 have mentioned these wormy integrowths as a result of pyroxferroite mesostasis [1-3], but there have been no detailed investigations of these textures. Similar mesostasis textures have been observed in only a few other lunar baslts (e.g.,14053 [4], 10044 [5], MIL 05035 [6], CE5 basalt clast (406-010,023) [7]). This dearth of data is partially due to the scale at which this texture is found and the means by which to observe it: only at a sub 100 micrometer scale using BSE microscopy can one see these symplectites. The implactions of this texture can provide information about the crystallization history of this sample and about the conditions at which this rock formed.

Background: Pyroxferroite has been experimentally shown to be metastable at low pressures with respect to the three-phase mineral assemblage of calcium-rich clinopyroxene, fayalite, and cristobalite. It crystallizes between 10-17.5 kbar and 1130-1250 ºC [8,9]. Experiments also demonstrated a volume reduction as pyroxferroite breaks down, which is consistent with the void spaces (Fig 1C) [8,10]. Experiments indicate that 12031 could have cooled to ≤990 ºC over 72 hours [10]. **12031 has preserved the breakdown of pyroxferroite before it went to completion.**

Observations: Sample 12031,40 is replete with this texture as almost every occurrence pyroxferroite crystal demonstrating this breakdown; 12031, 45 also has some occurrences, but to a lesser extent as it underwent significant laser ablation for analysis causing many crystals to be destroyed.

Both thin sections exhibit similar textures consisting of finer crystals with a preferred orientation in the center of the section, with coarser crystals on the rims that lack any preferred orientation. This textural variation could be indicative of a lava flow feature, but the very presence of the breakdown texture suggests that the sample is hypabyssal and not a surface flow. The pyroxferroite breakdown only found in the coarser crystals near the rims. One explanation for this variation could be that the sample experienced a two-stage cooling and that pyroxferroite only crystallized in the initial cooling regime and began to subsequently break down. Another explanation is that pyroxferroite is present in a xenolith that formed at depth and was picked up by the ascending magma, brouth to lower pressure, and subsequently broke down.

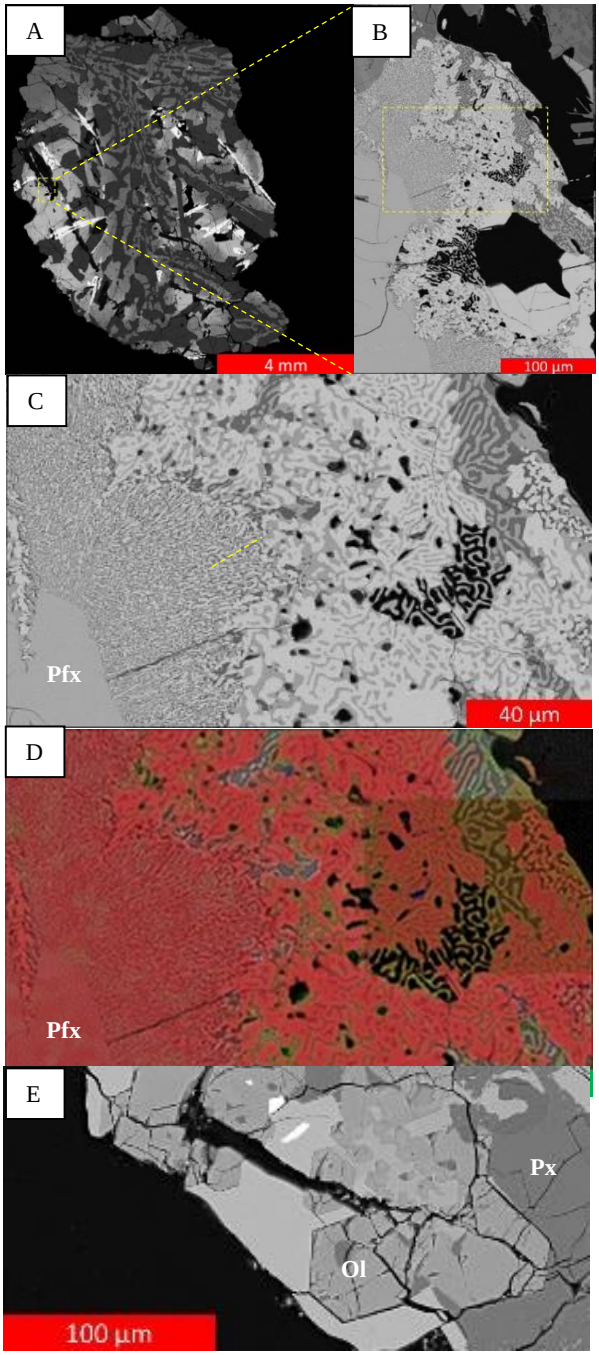

Figure 1*. Back-scattered electron images (BSE) of (A) 12031,30, (B) Zoomed in region (C) Symplectite texture where "Pfx" corresponds to Pyroxferroite, (D) Element map of (C) where iron is shown in red and calcium in green. The wormy intergrowths are calcium-rich while the pyroxferroite is iron rich, indicating a diffusion of calcium is one mechanism for this texture (E) Euhedral olivine crystals where "Ol" corresponds to Olivine and "Px" is iron-rich pyroxene endmember. The scale is incredibly fine, suggesting a brief, but slow cooling regime*

The breakdown texutres only occur on or around void spaces already present in the section, or in between mineral boundaries. The black areas in the BSE images are in fact void spaces and not silica-rich phases as could possibly be interpreted; the black vermicular intergrowths are thus void space created by the decrease in volume from the breakdown reaction [8,10]. The rest of the symplectite integrowths represent the different mineral phases that are reacting with one another.

Micron size euhedral fayalite crystals have also been observed in these sections (Figs. 2E, 3B). These are indicative of a rapid cooling regime before the minerals had time to grow large enough to make contact with one another.

The element map (Fig. 1E) is prediominantly iron rich with minor amounts of calcium. The iron is present in the pyroxferroite and fayalite phases while calcium is present in small amounts in pyroxferroite. The black regions, then, are void spaces and not silica phases. Stable iron-rich endmembers are present in this map, suggesting the breakdown occurred as the composition entered the "forbidden zone" of the pyroxene quadrilateral (as demarcated by the dashed line in Fig. 4) [6]. This texture, then, could be a result of calcium diffusion where it exits the pyroxferroite to form those intergrowths [11].

Conclusions: Pyroxferroite is metastable at the pressure below where it crystallized. The textures visible in this sample remarkably illustrate the mechanics of mineral breakdown. The variations in crystal sizes and locations of the mesostasis textures seem to suggest a two-stage crystallization. Since the breakdown texture is only present in the coarser crystals and as there are two populations, it can be inferred that pyroxferroite only formed in the secondary cooling regime and began to subsequently break down. We believe that pyroxferroite areas of 12031 represent xenolithic material of hyperbyssal/plutonic Fe-rich magma that was incorporated into an erupting magma by ascending to the surface. The pyroxferroite breakdown, therefore, did not go to completion and is preserved in this sample.

Understanding the breakdown of pyroxferroite is uniquely preserved in 12031. Higher resolution imagery and element mapping is needed to fully document the breakdown process.

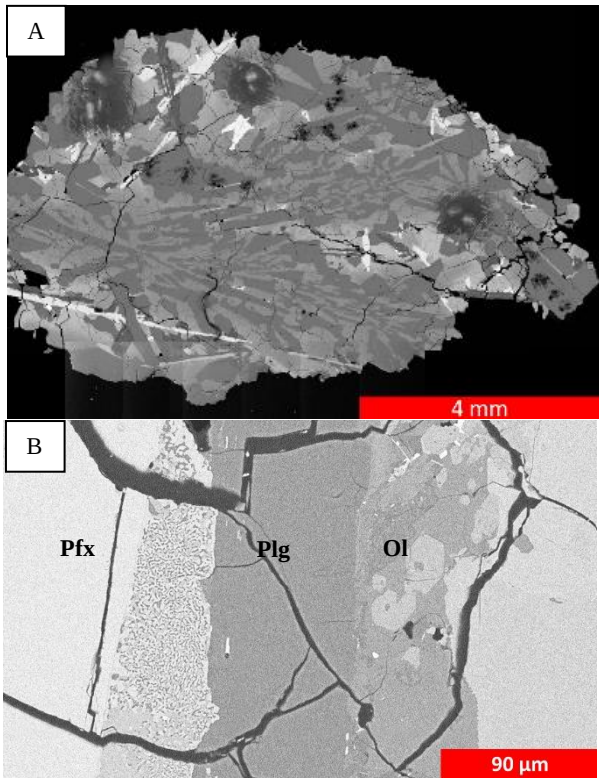

Figure 2. *BSE images of (A) 12031,45, (B) mesostasis texture between mineral grains where "Plg" represents plagioclase. Micrometer euhedral olivine is present in this section, analogous to section 40*

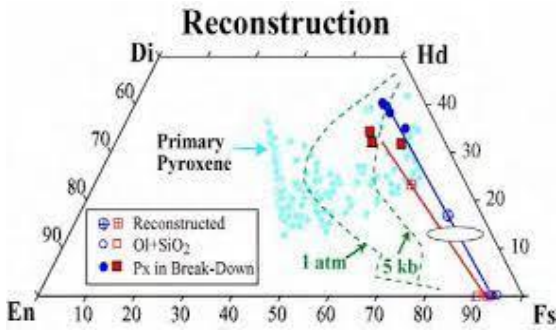

Figure 3. *Reconstruction of bulk composition of breakdown assemblages from Liu et al 2007 [6] The curved dashed lines mark the boundaries of the pyroxene "forbidden zone" where pyroxferroite begins to break down*

References: [1] Neal, C. R. et al (1994) *Meteoritics* 29, 334-348 [2] Meyer C. 12031 *Lunar Sample Compendium* [3] Beaty D.W. et al. (1979) *LPSC X* 115-139 [4] Taylor, L.A. et al (2004) *American Mineralogist* 89, 1617-1624. [5] Greenwood, J.P. et al. (2011) *Nature Geoscience* 4 79-82 [6] Liu, Y et al. (2007) *LPSC XXXVIII* [7] Hu, S. et al (2021) *Nature* 600, 49-53 [8] Lindsley, D.H. (1967) Carnegie Inst. Wash. Yearb. 65, 230-232; [9] Chao E.C.T. et al. (1970) Proc. Apollo 11 Lunar Sci. Conf. 65-79; [10] Lindsley D. H. et al. (1972) *LPSC III* 483-485 [11] Herd, C.D.K et al (2001) *LPSC XXXII*